JOURNAL OF THERMOPHYSICS AND HEAT TRANSFER
Vol. 8, No. 1, Jan.–March 1994

Combined Forced-Convection and Correlated-Radiation Heat Transfer in Cylindrical Packed Beds

K. Kamiuto* and S. Saitoh†
Oita University, Oita 870-11, Japan

The heat transfer characteristics of a fully developed forced convection flow in a cylindrical packed column at high temperatures are examined. The effects of non-Darcy and variable porosity are considered in the momentum equation, while the effects of radial thermal dispersion, variable effective thermal conductivity, and thermal radiation are taken into account in the energy equation. A new lateral mixing function is introduced to represent radial thermal dispersion coefficient. Radiative transfer in the packed bed is analyzed by utilizing the P_1 approximation and the correlated-radiative properties of packed spheres. After confirming the adequacy of the proposed heat transfer model, the effects of several system parameters on temperature profiles and heat transfer characteristics in cylindrical packed beds are examined in some detail.

Nomenclature

C = inertial coefficient
c_p = specific heat
Da = Darcy number
d_p = particle diameter
E_u = dimensionless pressure gradient
Fh = Forchheimer number
G = incident radiation
$\tilde{g}_s$ = asymmetry factor of the surface-scattering phase function
h_x = local heat transfer coefficient
$I(r, \Omega)$ = intensity of radiation
K = permeability
k_d = thermal dispersion conductivity of a packed bed
k_e = effective thermal conductivity of a packed bed
k_f = thermal conductivity of fluid
k_s = thermal conductivity of particles
N_R = conduction-radiation parameter
Nu_m = mean Nusselt number
Nu_ξ = local Nusselt number
n_p = number density of particles
P = pressure
Pr = Prandtl number
$\boldsymbol{q}$ = radiative heat flux vector
q_r = radial component of the radiative heat flux vector
Re = Reynolds number based on the diameter of a packed column
Re_p = local particle Reynolds number
r = radial coordinate
r_0 = radius of a cylindrical packed column
T = temperature
T_{0c} = inlet temperature of the fluid at the center of the bed
T_m = mean fluid temperature
T_w = wall temperature
T_0 = inlet temperature of the fluid
U = dimensionless axial velocity
u = axial velocity
u_m = mean axial velocity
x = axial coordinate
z = quantity defined by $(r_0 - r)/d_p$
$\tilde{\beta}$ = scaled extinction coefficient of a packed bed
Γ = ratio of the radius of a packed column to the particle diameter
γ_d = lateral mixing function
γ_2 = optical thickness ratio
ε_w = total hemispherical emissivity of the wall
ζ = dimensionless distance from the wall
η = dimensionless radial coordinate
θ = dimensionless temperature
θ_m = dimensionless mixing cup temperature
θ_0 = dimensionless inlet fluid temperature
κ = ratio of thermal conductivity of the solid to that of the fluid
λ_d = dimensionless thermal dispersion conductivity
λ_e = dimensionless effective thermal conductivity of a packed bed
μ = viscosity of fluid
ν = kinematic viscosity of fluid
ξ = dimensionless axial coordinate
ρ = density of fluid
ρ_s = hemispherical reflectivity of particles
ρ_w = hemispherical reflectivity of the wall
σ = Stefan-Boltzmann's constant
σ_a = absorption coefficient of a packed bed
$\tilde{\tau}_0$ = scaled optical thickness
ϕ = porosity
χ = dimensionless incident radiation
ψ = dimensionless radial radiative heat flux
Ω = direction of propagation of the light
$\tilde{\omega}$ = scaled albedo
$*$ = dimensionless quantity

Subscript
∞ = quantity at $\phi = 0.39$

Introduction

STUDIES of heat and fluid flow through packed beds have received much attention in relation to thermal designs of chemical reactors and regenerative heat exchangers, and a considerable number of experimental and analytical reports have been accumulated during the past few decades and summarized in several review articles.[1,2] However, almost all of these earlier studies were aimed at establishing semiempirical formulas for wall heat transfer coefficients and effective radial thermal conductivities on the basis of the lumped parameter

Received Aug. 26, 1992; revision received Jan. 4, 1993; accepted for publication Jan. 5, 1993.

*Professor, Department of Production Systems Engineering, Dannoharu 700.

†Graduate Student, Department of Production Systems Engineering.

model, assuming a plug flow with a constant transverse thermal dispersion, and were not directed toward accurate prediction of heat-transfer characteristics of packed beds based on a sound theoretical model incorporating the radial variations in temperature and velocity within the packed beds.

Recently, to circumvent this deficiency, the distributed parameter model considering boundary friction, inertial, nonhomogeneous and thermal dispersion effects have been developed by Vafai-Tien,[3] Cheng-Zhu,[4] Hunt-Tien,[5] and Hsu-Cheng[6] and have been successfully applied to forced-convection heat transfer problems in various packed beds. However, the effects of thermal radiation on packed-bed heat transfer have not yet been clarified in these previous studies. Under this circumstance, the major purpose of the present study is to examine the heat transfer characteristics of a fully developed forced-convection flow in cylindrical packed beds heated with elevated constant wall temperature. The Darcy-Brinkman-Ergun model is used for the momentum equation, with the radial porosity variations considered. The effects of radial thermal dispersion and variable stagnant effective thermal conductivities are taken into account in the energy equation. A new lateral mixing function is introduced so as to reproduce previous theoretical results for radial thermal dispersion coefficient, and Bruggeman's theory is utilized for evaluating the stagnant effective thermal conductivities. Moreover, radiative heat transfer through the packed beds is analyzed utilizing the P_1 approximation and our correlated-scattering theory for opaque packed spheres.[7]

Governing Equations

If we assume that 1) the packed bed is in local thermal equilibrium; 2) the flowfield in the packed bed is fully developed; 3) viscous dissipation and axial conduction terms in the energy equation have been neglected; 4) radiative heat transfer in the flow direction is negligible compared with radial radiation heat transfer[8]; and 5) the relevant radiative properties of the packed bed do not depend on the wavelength and the temperature, the steady-state governing equations including the radiation term are

$$\frac{\partial u}{\partial x} = 0 \tag{1}$$

$$\frac{\mu}{K}u + \rho C u^2 = -\frac{dP}{dx} + \frac{\mu}{\phi}\frac{1}{r}\frac{\partial}{\partial r}\left(r\frac{\partial u}{\partial r}\right) \tag{2}$$

$$\rho c_p u \frac{\partial T}{\partial x} = \frac{1}{r}\frac{\partial}{\partial r}\left[r(k_e + k_d)\frac{\partial T}{\partial r}\right] - \text{div } \boldsymbol{q}_R \tag{3}$$

$$\text{div } \boldsymbol{q}_R = \sigma_a(4\sigma T^4 - G) \tag{4}$$

where u and P are the velocity in the axial direction and pressure and ϕ is the local porosity. K and C represent the permeability and inertial coefficients and are given by

$$K = d_p^2\phi^3/150(1-\phi)^2 \tag{5}$$

$$C = 1.75(1-\phi)/d_p\phi^3 \tag{6}$$

The boundary conditions for Eqs. (1–3) are

$$\begin{aligned} &r = 0: \quad \frac{\partial u}{\partial r} = \frac{\partial T}{\partial r} = 0 \\ &r = r_0: \quad u = 0, \quad T = T_w \\ &x = 0: \quad T = T_0(<T_w) \end{aligned} \tag{7}$$

In addition to Eqs. (1–3), the equation of transfer[9] governing the intensity of radiation $I(r, \boldsymbol{\Omega})$ must also be solved, since Eq. (3) involves the incident radiation defined by $\int_{4\pi} I(r, \boldsymbol{\Omega})\, d\Omega$. For this purpose, we utilize the first-order spherical harmonic method (P_1 approximation).[10,11] The P_1 approximation has been proved to be valid, as long as optical thickness of a medium is sufficiently large[11]: this is true for the present case. The P_1 equations[10,11] are written as

$$\frac{\partial q_r}{\partial r} + \frac{q_r}{r} + \tilde{\beta}(1-\tilde{\omega})(G - 4\sigma T^4) = 0 \tag{8}$$

$$\frac{\partial G}{\partial r} + 3\tilde{\beta}(1 - \tilde{\omega}\tilde{g}_s)q_r = 0 \tag{9}$$

These equations are subject to the following boundary conditions:

$$\begin{aligned} &r = 0: \quad \frac{\partial G}{\partial r} = 0 \quad (\text{or } q_r = 0) \\ &r = r_0: \quad -(1-\rho_w)\frac{G}{4} + (1+\rho_w)\frac{q_r}{2} = -\varepsilon_w\sigma T_w^4 \end{aligned} \tag{10}$$

Dimensionless Governing Equations

We introduced the following dimensionless quantities to rewrite the governing equations in the dimensionless form:

$$C^* = \frac{C}{C_\infty}, \quad Da = \frac{K_\infty}{r_0^2}, \quad E_u = -\frac{dP}{dx}\Big/\left(\frac{\rho u_m^2}{r_0}\right), \quad Fh = C_\infty r_0$$

$$K^* = \frac{K_\infty}{K}, \quad N_R = \frac{k_f}{4\sigma T_w^3 r_0}, \quad Pr = \frac{\mu c_p}{k_f}, \quad Re = \frac{2u_m r_0}{\nu}$$

$$U = \frac{u}{u_m}, \quad \Gamma = \frac{r_0}{d_p}, \quad \eta = \frac{r}{r_0}, \quad \theta = \frac{T}{T_w}, \quad \theta_0 = \frac{T_0}{T_w} \tag{11}$$

$$\lambda_d = \frac{k_d}{k_f}, \quad \lambda_e = \frac{k_e}{k_f}, \quad \xi = \frac{(x/2r_0)}{RePr}, \quad \tilde{\tau}_0 = \tilde{\beta}r_0$$

$$\chi = \frac{G}{\sigma T_w^4}, \quad \psi = \frac{q_r r_0}{k_f T_w}, \quad \tilde{\omega} = 1 - \frac{\sigma_a}{\tilde{\beta}}$$

Introducing these dimensionless quantities yields the governing equations of the form

$$\frac{1}{2}E_u Re = \frac{K^*}{Da}U + \frac{1}{2}C^* FhReU^2 - \frac{1}{\phi}\frac{1}{\eta}\frac{\partial}{\partial\eta}\left(\eta\frac{\partial U}{\partial\eta}\right) \tag{12}$$

$$\frac{1}{4}U\frac{\partial\theta}{\partial\xi} = \frac{1}{\eta}\frac{\partial}{\partial\eta}\left[\eta(\lambda_e + \lambda_d)\frac{\partial\theta}{\partial\eta}\right] - \left[\tilde{\tau}_0\frac{(1-\tilde{\omega})}{N_R}\right]\left(\theta^4 - \frac{\chi}{4}\right) \tag{13}$$

The equation of the continuity may be represented in the following integral form:

$$2\int_0^1 U\eta\, d\eta = 1 \tag{14}$$

The relevant boundary conditions can be rewritten as

$$\begin{aligned} &\eta = 0: \quad \frac{\partial U}{\partial\eta} = \frac{\partial\theta}{\partial\eta} = 0 \\ &\eta = 1: \quad U = 0, \quad \theta = 1 \\ &\xi = 0: \quad \theta = \theta_0 \end{aligned} \tag{15}$$

The P_1 equations may also be rewritten in the dimensionless form

$$\frac{\partial\psi}{\partial\eta} + \frac{\psi}{\eta} + \left(\frac{\tilde{\tau}_0}{N_R}\right)(1-\tilde{\omega})\left(\frac{\chi}{4} - \theta^4\right) = 0 \tag{16}$$

$$\frac{\partial \chi}{\partial \eta} + 12N_R\tilde{\tau}_0(1 - \tilde{\omega}\tilde{g}_s)\psi = 0 \tag{17}$$

The boundary conditions for Eqs. (16) and (17) are

$$\eta = 0: \quad \frac{\partial \chi}{\partial \eta} = 0 \quad \text{or} \quad \psi = 0$$
$$\eta = 1: \quad -(1 - \rho_w)\frac{\chi}{4} + 2(1 + \rho_w)N_R\psi = -\varepsilon_w \tag{18}$$

Numerical Methods

The dimensionless governing equations were solved numerically by utilizing a finite difference scheme. The diffusion terms in the momentum and energy equations were approximated by a central difference scheme, while the convection term in the energy equation was represented by a backward difference scheme. The dimensionless radius of the packed bed was divided into 350 equally spaced increments for finite difference calculations. Finite difference equations derived from the momentum equation together with Eq. (14) constitute a set of simultaneous linear equations of 350 dimensions and were solved by Gaussian elimination, as the nonlinear term was treated as iterative ones. Utilizing the velocity distribution thus obtained, the discretized form of the energy equation was solved repeatedly until the prescribed convergence criterion was satisfied, as the radiation term and several of the diffusion terms were treated as iterative ones. At each step of iteration, the P_1 equations were also solved numerically to evaluate χ in Eq. (13) by finite differences using staggered lattice points. The details of this scheme were described elsewhere.[12] These solution procedures were carried out at each axial location while marching in the axial direction. Furthermore, to check the accuracy of the numerical calculations, several of the numerical results for the asymptotic Nusselt number, i.e., Nu_ξ at $\xi \to \infty$, in the case of pure forced-convection were compared with more accurate results which were obtained by utiliz-ing 2000 divisions for discretizing the energy equation. The comparison showed that the present results were about 1.5% smaller, in the worst case, than the more accurate results.

Heat Transfer Characteristics

The mixing cup temperature is evaluated by

$$T_m = 2\pi \int_0^{r_0} T(r)u(r)r \frac{dr}{\pi r_0^2 u_m} \tag{19}$$

and may be rewritten in the dimensionless form

$$\theta_m = 2\int_0^1 U\theta\eta \, d\eta \tag{20}$$

The local total heat transfer coefficient is defined by

$$h_x = \left[k_e \left.\frac{\partial T}{\partial r}\right|_{r=r_0} - q_r(r = r_0)\right] \Big/ (T_w - T_m) \tag{21}$$

Using this local heat transfer coefficient, the total Nusselt number may be evaluated as

$$N_{u_\xi} = h_x \cdot \frac{2r_0}{k_f} = 2\left[\left.\frac{\partial \theta}{\partial \eta}\right|_{\eta=1} - \psi(\eta = 1)\right] \Big/ (1 - \theta_m) \tag{22}$$

Physical Properties

Stagnant Effective Thermal Conductivity

The effective thermal conductivity which appears in Eq. (13) was evaluated utilizing Bruggeman's theory.[13] According to this theory, λ_e may be given by Eq. (23) for a gas-solid system

$$\lambda_e = k_e/k_f = (\kappa - 1)\kappa^{1/3}\phi[\sqrt[3]{(-1 + \sqrt{A})/2} - \sqrt[3]{(1 + \sqrt{A})/2}] + \kappa \tag{23}$$

where $A = 1 + (4/27)\phi^3(\kappa - 1)^3/\kappa^2$ and $\kappa = k_s/k_f$.

Thermal Dispersion Conductivity

k_d represents a degree of thermal transport due to the transverse mixing of local fluid streams within a packed bed and is generally represented in the form

$$\lambda_d = k_d/k_f = \gamma_d Pr Re_p \tag{24}$$

where Re_p is the local particle Reynolds number defined by $u(r)d_p/\nu$, and may be rewritten as

$$Re_p = ReU(\eta)/2\Gamma \tag{25}$$

γ_d in Eq. (24) is a lateral mixing function and has been assumed to be constant in the literature, but recently several authors[4,14] found that as long as γ_d is constant, the large temperature gradient near the heated wall cannot be reproduced and therefore they introduced a variable lateral mixing function. Very recently, Hsu and Cheng[6] theoretically formulated the radial dispersion coefficient utilizing the local volume-averaging technique for the energy equation. However, their formula involves an adjustable parameter to be determined posteriorly, and also is not related to previously reported theoretical values of γ_d as seen from Fig. 1. For this reason, we introduce a new lateral mixing function of the form

$$\gamma_d(\phi) = a(1 - \phi)^b \tag{26}$$

and determined values of a and b to reproduce two theoretical estimates of $\gamma_d(\phi)$ by Kunii[15] and Ranz,[16] i.e., $\gamma_d(0.7) = 0.02$ and $\gamma_d(0.26) = 0.179$. As a result, we obtained $a = 0.3718$ and $b = 2.4274$. The profile of the present lateral mixing function is shown by the solid line in Fig. 1, where Hsu-Cheng's correlation defined by $\gamma_d = 0.04(1 - \phi)/\phi$ is depicted by the broken line and the experimental data compiled by Yagi-Kunii-Wakao[17] are denoted by the open circles.

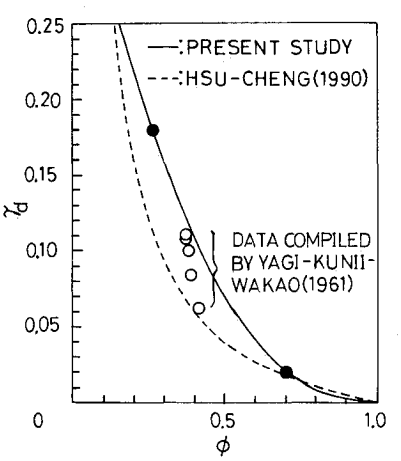

Fig. 1 Profiles of the lateral mixing functions.

Radiative Properties of a Packed Bed

Under usual packed bed conditions, i.e., $\phi \cong 0.4$, the radiative properties such as $\tilde{\tau}_0$, $\tilde{\omega}$, *and* $\tilde{g}_s$ cannot be represented by simply summing the radiative properties of individual spheres and, as pointed out by one of the authors,[7] correlation between scatterers must be taken into account. Utilizing a semi-empirical correlated-scattering theory,[7] the scaled radiative properties appropriate to a packed bed consisting of large diffuse spheres are described as follows:

$$\begin{aligned} \tilde{\tau}_0 &= \tilde{\beta} r_0 = (2\gamma_2 - 1)(\pi d_p^2 n_p/4) r_0 \\ &= 1.5\Gamma(2\gamma_2 - 1)(1 - \phi) \\ \tilde{\omega} &= \rho_s \\ \tilde{g}_s &= -\tfrac{4}{9} \end{aligned} \tag{27}$$

where γ_2 represents the optical-thickness ratio[7] and is given by

$$\gamma_2 = 1 + 1.5(1 - \phi) - (\tfrac{3}{4})(1 - \phi)^2 \tag{28}$$

If a packed bed consists of specular opaque spheres, then a value of $\tilde{g}_s$ must be estimated directly from the definition of the asymmetry factor of the surface-scattering phase function.

Porosity Distribution Function

To account for the porosity variations near the wall, Ridgeway-Tarbuck's experimental data[18] were approximated by the following expressions[19] and were utilized throughout the present study.

For $0 \leq \zeta \leq 0.6$

$$\phi(\zeta) = 1 - 3.10036\zeta + 3.70243\zeta^2 - 1.24612\zeta^3 \tag{29}$$

For $0.6 < \zeta \leq \Gamma$

$$\phi(\zeta) = -0.1865 \exp(-0.22\zeta_1^{1.5})\cos(7.66\zeta_1) + 0.39 \tag{30}$$

where $\zeta_1 = \zeta - 0.6$, $\zeta = z/d_p$, and z represents the distance from the wall. These expressions are expected to hold under the condition of $\Gamma \gtrsim 5$.

Results and Discussion

Velocity Profile and Hydrodynamic Characteristics

A typical velocity profile is shown in Fig. 2. The velocity profile oscillates periodically in accord with the radial porosity variation and this quantitative feature holds even for other Reynolds numbers, although the maximum velocity appearing near the wall increases with the Reynolds number.

Correlations between E_u^* and Re are shown in Fig. 3. The dimensionless pressure gradient becomes higher as Γ is increased, since Da and Fh are connected with Γ through the relations of $Da = 0.0010628/\Gamma^2$ and $Fh = 17.99592\Gamma$, and thus, the porous viscous and inertial terms in the momentum equation become notable with increase in Γ.

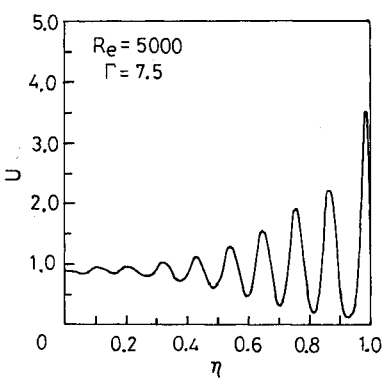

Fig. 2 Typical velocity profile within a cylindrical packed bed.

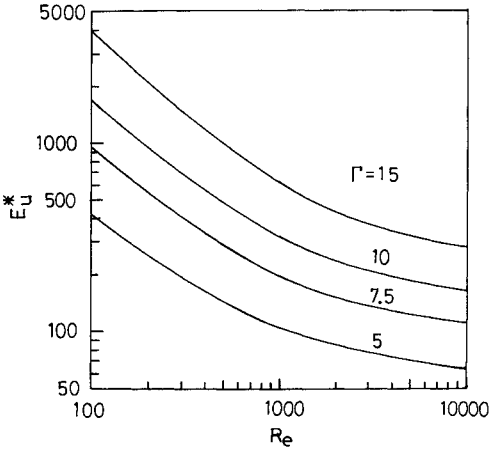

Fig. 3 Relations between the dimensionless pressure gradient and the Reynolds number.

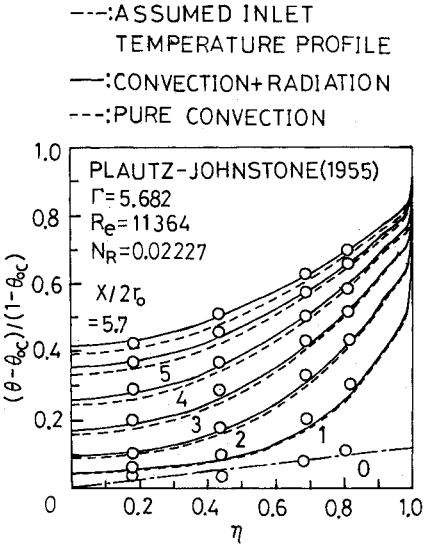

Fig. 4 Numerically calculated temperature profiles within a packed bed of glass beads.

Adequacy of the Heat Transfer Model

To examine the validity of the present heat transfer model, the energy equation and the P_1 equations are solved under conditions corresponding to the experiments made by Plautz and Johnstone[20] and Verschoor and Schuit[21] for forced-convection of air ($Pr = 0.705$) in cylindrical packed beds consisting of specular glass spheres. The physical properties of glass spheres were assumed to be $k_s = 1.05$ (W/mK), $\rho_s = 0.1$, and $\tilde{g}_s = 0.4063$. Figure 4 compares calculated temperature profiles with the experimental results obtained by Plautz and Johnstone[20] at various axial directions. In the analysis, the hemispherical emissivity of the heated steel wall was assumed to be 0.275[22] and the measured inlet temperatures were utilized instead of a uniform inlet fluid temperature. The solid lines in Fig. 4 show the numerical results obtained by taking into account the effects of radiation, while the broken lines are concerned with pure forced-convection. Calculated temperature profiles are characterized by the steep temperature gradient near the wall due to wall channeling effects and a reduction in the transverse thermal dispersion. As seen from this figure, the effects of thermal radiation become noticeable for increasing values of $x/2r_0$. Agreement between the present

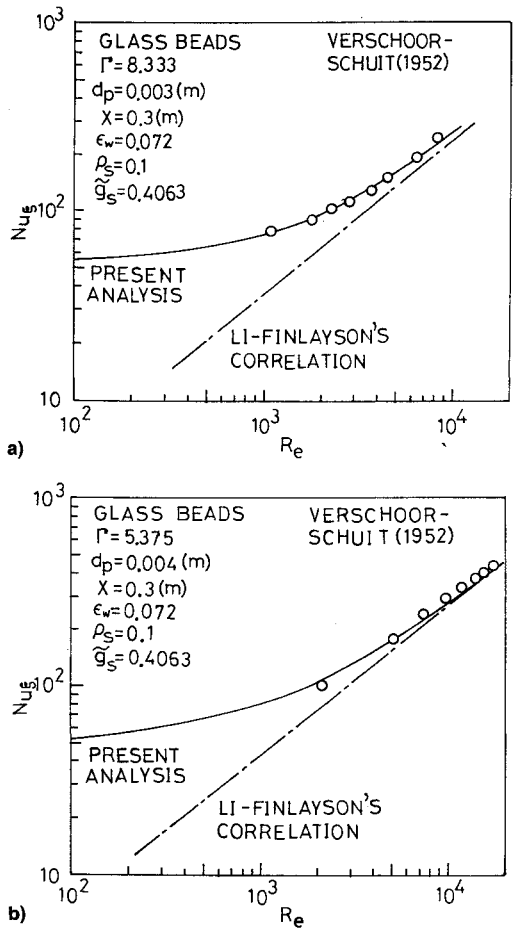

Fig. 5 Relations between the asymptotic Nusselt number and the Reynolds number for a packed bed of glass beads with a) $d_p = 0.003$ (m) and b) $d_p = 0.004$ (m).

numerical results and experimental data is quite excellent, and this substantiates the adequacy of the present thermal model.

Figures 5a and 5b compare predicted asymptotic Nusselt numbers, i.e., Nu_ξ at $\xi \to \infty$, with experimental results obtained by Verschoor and Schuit.[21] In the analysis, a uniform inlet temperature profile was assumed, and moreover, the hemispherical emissivity of the heated copper wall was assumed to be 0.072,[22] so that the effects of thermal radiation are scarcely observed: the difference between Nu_ξ, taking into account radiation and that for pure-convection, is always less than 0.5%. The dot-dashed line in these figures indicates the heat transfer correlation obtained by Li and Finlayson[1]

$$Nu_m = 2.03(Re/2\Gamma)^{0.8} \exp(-3/\Gamma) \tag{31}$$

It is noted that the present theoretical results for asymptotic Nusselt number agree well with the experimental data over a wide range of Re. On the other hand, agreement between Li-Finlayson's correlation and the experimental results is poor except for the high Reynolds number region.

Effects of System Parameters on Temperature Profiles and Heat Transfer Characteristics

Based on the present heat transfer model, it is possible to examine the effects of several system parameters on temperature profiles and heat transfer characteristics. To this end, we assume that 1) the cylindrical packed bed consists of diffuse solid particles with $\tilde{g}_s = -\frac{4}{9}$; 2) the heated wall is isothermal and black ($\varepsilon_w = 1.0$); 3) air ($Pr = 0.705$) is flowing through the bed column with $Re = 5000$; 4) the flowfield is fully developed at the inlet of the bed column; and 5) the temperature profile at the inlet is uniform and $\theta_0 = 0.75$. The range of the system parameters used in the present calculations is summarized in Table 1. This table also gives the key to Figs. 6 and 7. Typical temperature profiles at $\xi = 2 \times 10^{-4}$ are shown in Fig. 6 where the results for pure convection are denoted by the broken lines. The temperature profiles rise higher as N_R becomes small and the ratio of the thermal conductivities of the solid and fluid κ becomes large. When Γ is increased, the temperature fields establish more slowly in the flow direction. Relations between Nu_ξ and ξ are shown in Fig. 7. It is noted that, when the effects of thermal radiation is taken into account, the local Nusselt number decreases and reaches a minimum value at a certain axial location and then increases again with ξ. This feature agrees quantitatively with

Table 1 Key for Figs. 6 and 7

No.	Γ	κ	ρ	N_R
1	7.5	10	0.1	0.01
2	7.5	10	0.1	0.001
3	7.5	10	0.1	0.0001
4	7.5	100	0.1	0.001
5	10.0	10	0.1	0.001
6	7.5	10	0.9	0.001
7	7.5	10	1.0	∞
8	7.5	100	1.0	∞
9	10.0	10	1.0	∞

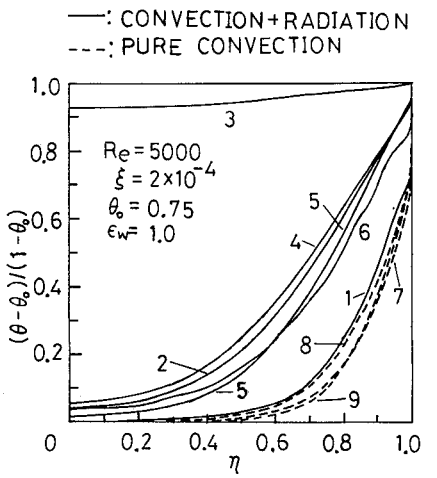

Fig. 6 Effects of several system parameters on the temperature profile within a packed bed. The key for this figure is given by Table 1.

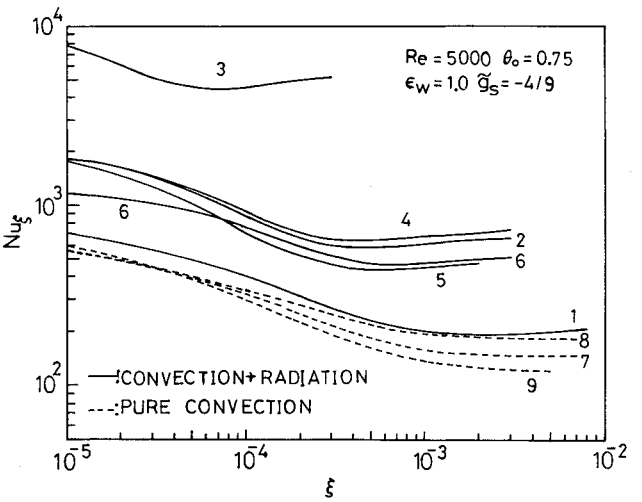

Fig. 7 Effects of several system parameters on the relation between the local Nusselt number and the dimensionless axial coordinate. The key for this figure is given by Table 1.

the trends for local Nusselt number reported in the literature for heat transfer by simultaneous radiation and convection in flowing radiating gases. This figure also shows that, at a given ξ, the local Nusselt number increases with decrease in N_R, ρ_s, and Γ, and with increase in κ. The effects of N_R and ρ_s on Nu_ξ are selfexplanatory because N_R is concerned with the wall temperature and ρ_s is directly related to the albedo governing the interaction between thermal radiation and packed spheres. On the other hand, the effects of κ and Γ on Nu_ξ need to be explained. λ_e increases with κ through Eq. (23), and thus an increase in κ results in an enhancement of convective heat transfer through a packed bed, i.e., an increase in Nu_ξ. However, this effect is not so appreciable as seen in Fig. 7. When Γ is increased, the wall channeling phenomenon diminishes and optical thickness becomes large, so that Nu_ξ decreases.

Concluding Remarks

The present study examines the heat transfer characteristics of a fully developed forced-convection flow in a cylindrical packed bed heated at high temperatures. The Darcy-Brinkman-Ergun model is used as the momentum equation, with the radial porosity variations considered. Energy equation includes the effects of variable stagnant thermal conductivity, radial thermal dispersion, and thermal radiation: the stagnant effective thermal conductivity is evaluated using Bruggeman's theory and a new lateral mixing function is formulated to represent the radial thermal dispersion conductivity quantitatively. The effects of thermal radiation are considered on the basis of the P_1 approximation and the correlated-radiative properties of packed spheres. The proposed heat transfer model is substantiated to quantitatively predict existing experimental data for temperature profiles and asymptotic Nusselt numbers. Moreover, with this heat transfer model, simultaneous forced-convection and radiation heat transfer in a cylindrical packed bed heated with constant wall temperature is analyzed and the effects of several system parameters such as N_R, ρ_s, Γ, and κ on temperature profiles and local Nusselt numbers are revealed. The proposed heat transfer model involves no free parameters that must be determined empirically, and may, therefore, be readily applied to other types of packed bed at high temperatures.

References

[1]Beek, J., "Design of Packed Catalytic Reactors," *Advances in Chemical Engineering*, Vol. 3, Academic Press, New York, 1962, pp. 203–271.

[2]Li, C. H., and Finlayson, B. A., "Heat Transfer in Packed Beds—A Reevaluation," *Chemical Engineering Science*, Vol. 32, pp. 1055–1066.

[3]Vafai, K., and Tien, C. L., "Boundary and Inertia Effects on Flow and Heat Transfer in Porous Media," *International Journal of Heat and Mass Transfer*, Vol. 24, No. 1, 1981, pp. 195–203.

[4]Cheng, P., and Zhu, H., "Effects of Radial Thermal Dispersion on Fully-Developed Forced Convection in Cylindrical Packed Beds," *International Journal of Heat and Mass Transfer*, Vol. 30, No. 11, 1987, pp. 2373–2382.

[5]Hunt, M. L., and Tien, C. L., "Non-Darcian Convection in Cylindrical Packed Beds," *Journal of Heat Transfer*, Vol. 110, May 1988, pp. 378–384.

[6]Hsu, C. T., and Cheng, P., "Thermal Dispersion in a Porous Medium," *International Journal of Heat and Mass Transfer*, Vol. 33, No. 8, 1990, pp. 1587–1597.

[7]Kamiuto, K., "Radiative Properties of Packed-Sphere Systems Estimated by the Extended Emerging-Intensity Fitting Method," *Journal of Quantitative Spectroscopy and Radiative Transfer*, Vol. 47, No. 4, 1992, pp. 257–261.

[8]Echigo, R., Hasegawa, S., and Kamiuto, K., "Composite Heat Transfer in a Pipe with Thermal Radiation of Two-Dimensional Propagation—in Connection with the Temperature Rise in Flowing Medium Upstream from Heating Section," *International Journal of Heat and Mass Transfer*, Vol. 18, No. 10, 1975, pp. 1149–1159.

[9]Mengüc, M. P., and Viskanta, R., "Radiative Transfer in Axisymmetric, Finite Cylindrical Enclosures," *Journal of Heat Transfer*, Vol. 108, May 1986, pp. 271–276.

[10]Cheng, P., "Two-Dimensional Radiating Gas Flow by a Moment Method," *AIAA Journal*, Vol. 2, No. 9, 1964, pp. 1662–1664.

[11]Harris, J. A., "Solution of the Conduction/Radiation Problem with Linear-Anisotropic Scattering in an Annular Medium by the Spherical Harmonic Method," *Journal of Heat Transfer*, Vol. 111, Feb. 1989, pp. 194–197.

[12]Kamiuto, K., Saitoh, S., and Itoh, K., "Numerical Model for Combined Conductive and Radiative Heat Transfer in Annular Packed Beds," *Numerical Heat Transfer, Part A*, Vol. 23, 1993.

[13]Kamiuto, K., "Examination of Bruggeman's Theory for Effective Thermal Conductivities of Packed Beds," *Journal of Nuclear Science and Technology*, Vol. 27, No. 5, 1990, pp. 473–476.

[14]Cheng, P., and Vortmeyer, D., "Transverse Thermal Dispersion and Wall Channeling in a Packed Bed with Forced Convection Flow," *Chemical Engineering Science*, Vol. 43, 1988, pp. 2523–2532.

[15]Kunii, D., *Thermal Unit Operations*, Vol. 1, Maruzen, Tokyo, 1976, p. 149.

[16]Ranz, W. E., "Friction and Transfer Coefficients for Single Particles and Packed Beds," *Chemical Engineering Progress*, Vol. 48, 1952, pp. 247–253.

[17]Yagi, S., Kunii, D., and Wakao, N., "Radially Effective Thermal Conductivities in Packed Beds," *International Developments in Heat Transfer*, Pt. III, American Society for Mechanical Engineers, New York, 1961, pp. 742–749.

[18]Ridgway, K., and Tarbuck, K. J., "Radial Voidage Variations in Randomly-Packed Beds of Spheres of Different Sizes," *Journal of Pharmacy and Pharmacology*, Vol. 18, Supplement, 1966, pp. 168S–175S.

[19]Kamiuto, K., Nagumo, Y., and Iwamoto, M., "Mean Effective Thermal Conductivities of Packed-Sphere Systems," *Applied Energy*, Vol. 34, 1989, pp. 213–221.

[20]Plautz, D. A., and Johnstone, H. F., "Heat and Mass Transfer in Packed Beds," *A.I.Ch.E. Journal*, Vol. 1, 1955, pp. 193–199.

[21]Verschoor, H., and Schuit, G. C. A., "Heat Transfer to Fluids Flowing Through a Bed of Grannular Solids," *Applied Scientific Research*, Vol. A2, 1952, pp. 97–119.

[22]McAdam, W. H., *Heat Transmission*, McGraw-Hill-Kogakusha, Tokyo, 1986, Table A-23.